Shallow trap modelling of infrared sensitive 'blue' $BaTiO_3$

Graeme W. Ross and Robert W. Eason

Optoelectronics Research Centre and Department of Physics

University of Southampton, Southampton, SO9 5NH, U.K.

M. J. Damzen, R. Ramos-Garcia and R. C. Troth

The Blackett Laboratory, Imperial College

Prince Consort Road, London SW7 2BZ, U.K.

Mark H. Garrett* and Daniel Rytz

Sandoz Huningue S.A., Centre de Recherche en Optoélectronique

Avenue de Bâle, 68330 Huningue, France

Abstract

We present experimental data for the intensity-dependent absorption coefficient of a photorefractive "blue" sample of rhodium-doped $BaTiO_3$ using beams of different wavelengths. A numerical photorefractive two-level model incorporating dual-wavelength illumination and a secondary photorefractive centre gives good agreement with experiment. We deduce values for the number densities, photoionisation cross-sections, thermal ionisation rate and recombination coefficients of the photorefractive centres. In this sample we determine that there is the usual deep trap concentration of $\sim 2 \times 10^{16} cm^{-3}$ and a relatively high shallow trap density of $\sim 1 \times 10^{18} cm^{-3}$.

* Present address : Deltronic Crystal Industries, Inc., 60 Harding Avenue, Dover NJ 07801, USA

The photorefractive crystal $BaTiO_3$ has been the subject of many experimental and theoretical investigations due to its attractive nonlinear optical properties, which permit high two-beam coupling gain and high self-pumped phase conjugate reflectivities without the need for an externally applied electric field. Past research on the photorefractive properties of $BaTiO_3$ has focused on its response in the visible spectrum where it has been most sensitive. Much interest has recently turned towards near-infrared wavelengths compatible with diode-pumped solid state lasers and semiconductor lasers with applications such as diode injection locking [1] and brightness enhancement [2].

Infrared sensitive $BaTiO_3$ has been reported recently [3] using crystals, blue in colour, which possess enhanced absorption in the red and near infrared regions of the spectrum. Figure 1 shows the absorption spectrum of such a sample together with a nominally undoped sample of $BaTiO_3$ for comparison. Recent attempts to identify the impurity responsible for the blue colour and the dominant photorefractive centre has suggested that rhodium (in the valences states Rh^{3+}/Rh^{4+}) may be responsible [4,5]. Through systematic addition of rhodium to the crystal melt, Wechsler [5] and his colleagues obtained crystals which shared not only a remarkably similar absorption profile to that shown in figure 1, but also similar optical and photorefractive characteristics to those reported in reference 3. In our crystal of $BaTiO_3$ both Rh and Fe were determined to be present by Spark Source Mass Spectroscopy [6] and Electron Paramagnetic Resonance [7].

In this paper, we present results of intensity-dependent absorption in an infrared sensitive "blue" sample of $BaTiO_3$:Rh. The photoinduced absorption change indicates the presence of secondary photorefractive centres [8-13]. By using dual-wavelength illumination of the sample and by exploiting the wavelength dependence of the photoionisation cross section of the photorefractive centres, we have been able to model the results. We used a

two-centre (deep and shallow trap) model modified to incorporate simultaneous illumination by two different wavelength.

It has been shown that the intensity-dependent absorption is consistent with the presence of secondary centres [8,9]. These are intermediate-level charge trapping impurity sites that are usually highly ionised at room temperature, but can be populated by photoionised charge carriers from the deep centres. The photoinduced transfer of charge from a deep to a secondary centre leads to a change in the absorption of the crystal due to different photoionisation cross-sections and concentrations of these centres. Previous photoinduced measurements [10] involve the transmission of a weak incoherent beam through a photorefractive crystal to monitor the changes in the absorption induced by varying a strong pump beam. In this paper we vary the intensity of both beams which are at different wavelengths and extend the two-centre photorefractive model to include this feature.

A model that incorporates the secondary centres and dual-wavelength illumination is shown schematically in figure 1. In our notation N and N^+ are the densities of the deep centres with total deep centre density $N_D=N+N^+$, M and M^+ are the densities of shallow centres with total shallow centre density $M_T=M+M^+$. The parameters S, β, and γ are, respectively, the cross-section for photoionisation, rate of thermal ionisation and coefficient of recombination. The un-subscripted parameters refer to the deep centres and the corresponding parameters with subscript S refer to secondary-trap coefficients. I_1 and I_2 are the intensities of beams 1 and 2 with wavelength λ_1 and λ_2, respectively.

The material equations for the two-centre model have been presented previously [8,9]. To introduce the two wavelength illumination we note that beams 1 and 2 are incoherent so no beam coupling is observed, and the presence of the second beam can be simply represented by an intensity dependent contribution to the thermal ionisation rates of the deep

and secondary centres and given by

$$\beta(I_2)=\beta+S(\lambda_2)I_2 \tag{1}$$

$$\beta_S(I_2)=\beta_S+S_S(\lambda_2)I_2 \tag{2}$$

where $S(\lambda_2)I_2$ and $S_S(\lambda_2)I_2$ are the photoionisation rates due to beam 2. To calculate the intensity dependence of the absorption coefficient, we assumed uniform illumination on both beams, set the electric field and current to zero in the material equations, and solved them in steady-state. The absorption coefficient at wavelength λ_1 due to the presence of both beams is given then by the formula [9]

$$\alpha(I_1,I_2)=\alpha(0)+\frac{hc}{\lambda}[S_S(\lambda_1)-S(\lambda_1)]M^+(I_1,I_2) \tag{3}$$

where $\alpha(0)$ is the low intensity absorption coefficient when $I_1=I_2=0$, and $M^+(I_1,I_2)$ is the population of shallow traps filled with holes due to photoinduced transfer of charge from the deep levels and is a saturating function of intensity [9]. Analysis shows that strong intensity-induced filling of the secondary centres occurs at a characteristic saturation intensity given by $I_{sat}=\beta_S/S_S$ [9,12]. It is noted that due to the wavelength dependence of S_S, I_{sat} is also wavelength dependent. With dual wavelength illumination the parameter β_S can also be made intensity dependent according to equation 2.

The first experiment to test photoinduced absorption was arranged by measuring the transmission of an o-polarised He-Ne through the blue $BaTiO_3$ crystal sample with dimensions 7.3x3.0x5.6mm^3 (with the c-axis parallel to the 5.6mm edge - see inset of figure 3). Figure 3 shows a plot of the absorption with the incident He-Ne intensity. The graph indicates an intensity dependent reduction of the absorption coefficient corresponding to light-induced transparency with $S_S(\lambda_1)<S(\lambda_1)$ [13]. This is the reverse effect compared to

observations in as-grown $BaTiO_3$ samples [8], where an intensity dependent induced increase in absorption have been observed ($S_S(\lambda_1) > S(\lambda_1)$). The solid line shown in figure 3 is a theoretical curve using a numerical simulation of the model described in the previous section and using the parameters listed in table 1.

In a second experiment the crystal was illuminated by two beams, an o-polarised He-Ne beam at $\lambda_1 = 633$nm and an o-polarised near-infrared beam at $\lambda_2 = 800$nm produced by a Ti:sapphire laser. The arrangement of the beams was as shown in figure 4 and, once again, the use of o-polarised beams minimised photorefractive grating effects. The He-Ne laser beam was fixed at intensity $I_1 = 0.85 Wcm^{-2}$ which corresponded to a strongly saturated condition of the induced transparency according to figure 3. The change in transmission of the He-Ne beam was then monitored as a function of the intensity I_2. The graphs in figure 4 show the change in the absorption coefficient as a function of the near-infrared illumination I_2 for the two cases of $\lambda_2 = 800$ and 750nm. According to equation 3, the dual-wavelength change in absorption coefficient in this case can be written as $\Delta\alpha(I_2) = \alpha(I_1 = 0.85 Wcm^{-2}, I_2) - \alpha(I_1 = 0.85 Wcm^{-2}, 0)$. The solid and dashed curves show the theoretical modelling for $\lambda = 800$nm and $\lambda = 750$nm respectively using, the parameters listed in table 1.

A summary of the crystal parameters used in our numerical simulations is shown in table 1, and were deduced from our measurements. By measuring the two-beam coupling gain coefficient as a function of the grating wavevector (using a wavelength of 647nm and total intensity of $0.27 Wcm^{-2}$) we estimated the effective trap density to be $N_{eff}(\sim N) \sim 2 \times 10^{16} cm^{-3}$. The wavelength-dependent absorption coefficient at low intensity $\alpha_0(\lambda) \approx (hc/\lambda) S(\lambda) N^+$ due to hole photoionisation from the dark value of the positively-charged deep centre species ($N^+ = N_A$), can be used to determine the cross-section for photoionisation. From the intensity dependent absorption data shown in figure 3, we

determine the characteristic saturation intensity for shallow trap filling as $I_{sat}=\beta_S/S_S \sim 22 mWcm^{-2}$ at $\lambda_1=633nm$. Dark decay measurements of the observed changes in the absorption were characterised by an initial rapid decrease followed by a slow recovery (a few seconds) as observed in the experiments of Brost and Motes [10]. The time scales of the process was intensity-dependent: occurring faster for higher intensities, in agreement with previous observations [11]. From the measured time of dark decay recovery of induced absorption $\sim$ 10-12s, we estimate $\beta_S \sim 0.1 s^{-1}$. With these parameters we found fitted values for the photoionisation cross section $S_S \sim 13.4 cm^2 J^{-1}$ at $\sim$ 633nm and total density of shallow traps $M_T \sim 1.1 x 10^{18} cm^{-3}$.

In order to verify consistency of our model with these parameters, we modelled the dark decay measurements of the induced absorption. Our model predicted a dark decay time of $\sim$ 10 s, in correspondence with the experiment. Additionally the modelling of dark decay allows us to estimate the magnitude of the shallow trap recombination to deep trap recombination γ_S/γ since the temporal behaviour of dark decay of the change in absorption coefficient ($\propto M^+$) is given by the following equation

$$\frac{\partial M^+}{\partial t} = -\frac{\beta_S M^+}{1+\gamma_S M/\gamma N} \qquad (4)$$

where $M=M_T-M^+(t)$ and $N=N_D-N_A+M^+(t)$ are time dependent and the decay will be non-exponential in form. The ratio $\gamma_S M/\gamma N$ is physically equal to the average number of times the thermally-ionised carrier from a filled shallow level is retrapped back into the shallow trap before it recombines with a deep trap. From equation 4, it can be seen that the exponential decay time (τ_D) measured experimentally is an approximation to the reciprocal of a weighted time-average decay rate and therefore within the limits $\beta_S/(1+\gamma_S M_T/\gamma(N_D-N_A)) < \tau_D^{-1} < \beta_S$.

Once we have characterised the shallow trap at a given wavelength we can easily find the values of the cross-section for photoionisation at any second wavelength with the help of the absorption spectrum and by fitting the change in the absorption coefficient $\Delta\alpha$ to experimental data. This method reproduces quantitatively good results at infrared wavelengths when we extended the model to visible regions of the spectrum we found only qualitatively agreement. We speculate that other effects not included in this model such as electron-hole competition [14] and multiple shallow trap levels [15] may cause deviations of the experimental results from the present model.

In summary, results of dual-wavelength intensity dependent absorption measurements using infrared sensitive $BaTiO_3$ have been modelled numerically and used to identify deep and secondary centre parameters. The good agreement between experiment and theory, which uses a common set of parameters to model all cases, indicates that the two-centre model seems to be adequate to explain the intensity dependent behaviour of our rhodium-doped $BaTiO_3$ in the red and near-infrared spectral regions.

This work was supported by funding from the Carnegie Trust for the Universities of Scotland and from the Science and Engineering Research Council (SERC). We thank the Rutherford Appleton Laboratory, Chilton, Didcot, UK for the Ti:sapphire laser used in this research.

References

1 S. MacCormack, J. Feinberg and M. H. Garrett, CLEO Technical Digest **11**, CThS55 (1993)

2 S. MacCormack and J. Feinberg, CLEO Technical Digest **11**, CTuN 19 (1993)

3 G. W. Ross, P. Hribek, R.W. Eason, M. H. Garret and D. Rytz, Opt.Commun. **101**, 60 (1993)

4 C. Warde, T. W. McNamara, M. H. Garrett and P. Tayebati, SPIE Conference, San Diego CA, CR48-07 (1993)

5 B. A. Wechsler, M. B. Klein, C. C. Nelson and R. N. Schwartz, Opt.Lett. **19**, 536 (1994)

6 M. H. Garrett, H. P. Jenssen, C. Warde, G. D. Bacher, S. MacCormack, J. Feinberg and R. N. Schwartz, "Characterisation of the infrared photorefractive response of rhodium-doped 'blue' $BaTiO_3$", submitted to J.Opt.Soc.Am.B, 1994

7 EPR measurements made by R. N. Schwartz, Hughes Research Lab, Malibu, CA

8 G. A. Brost, R. A. Motes and J. R. Rotgé, J.Opt.Soc.Am. B **5**, 1879 (1988)

9 P. Tayebati and D. Mahgerefteh, J.Opt.Soc.Am. B **8**, 1053 (1991)

10 G. A. Brost and R. A. Motes, Opt.Lett. **15**, 538 (1990)

11 R. A. Motes, G. A. Brost, J. R. Rotgé and J. J. Kim, Opt.Lett. **13**, 509 (1988)

12 D. Mahgerefteh and J. Feinberg, Phys. Rev. Lett. **64**, 2195 (1990)

13 M. H. Garrett, P. Tayebati, J. Y. Chang, H. P. Jenssen and C. Warde, J.Appl.Phys. **72**, 1965 (1992)

14 G. C. Valley, J.Appl.Phys. **59**, 3363 (1986)

15 R. S. Cudney, R. M. Pierce, G. D. Bacher and J. Feinberg, J.Opt.Soc.Am. B **8**, 1326 (1991)

Figure Captions

Figure 1 Absorption spectrum of the infrared-sensitive $BaTiO_3$ using light polarised parallel to the crystal c-axis. The spectrum of typical $BaTiO_3$ crystal is shown in dashed line (crystal A) and the spectrum of the infrared-sensitive $BaTiO_3$ is shown in solid line (crystal B).

Figure 2 Model diagram of photorefractive infrared-sensitive $BaTiO_3$ with deep and secondary (shallow) centres and two wavelength illumination.

Figure 3 Intensity-dependence of the absorption coefficient showing light induced transparency at 633nm. The filled dots are experimental data and solid curve is theoretical simulation based on the parameters of table 1.

Figure 4 Change in the absorption coefficient at 633nm with fixed intensity I_1 as a function of the infrared intensity I_2 at two different wavelengths. Filled dots (λ_2=800nm) and open dots (λ_2=750nm) are experimental data. Solid line (λ_2=800nm) and dashed line (λ_2=750nm) are theoretical curves based on the parameters given in table 1.

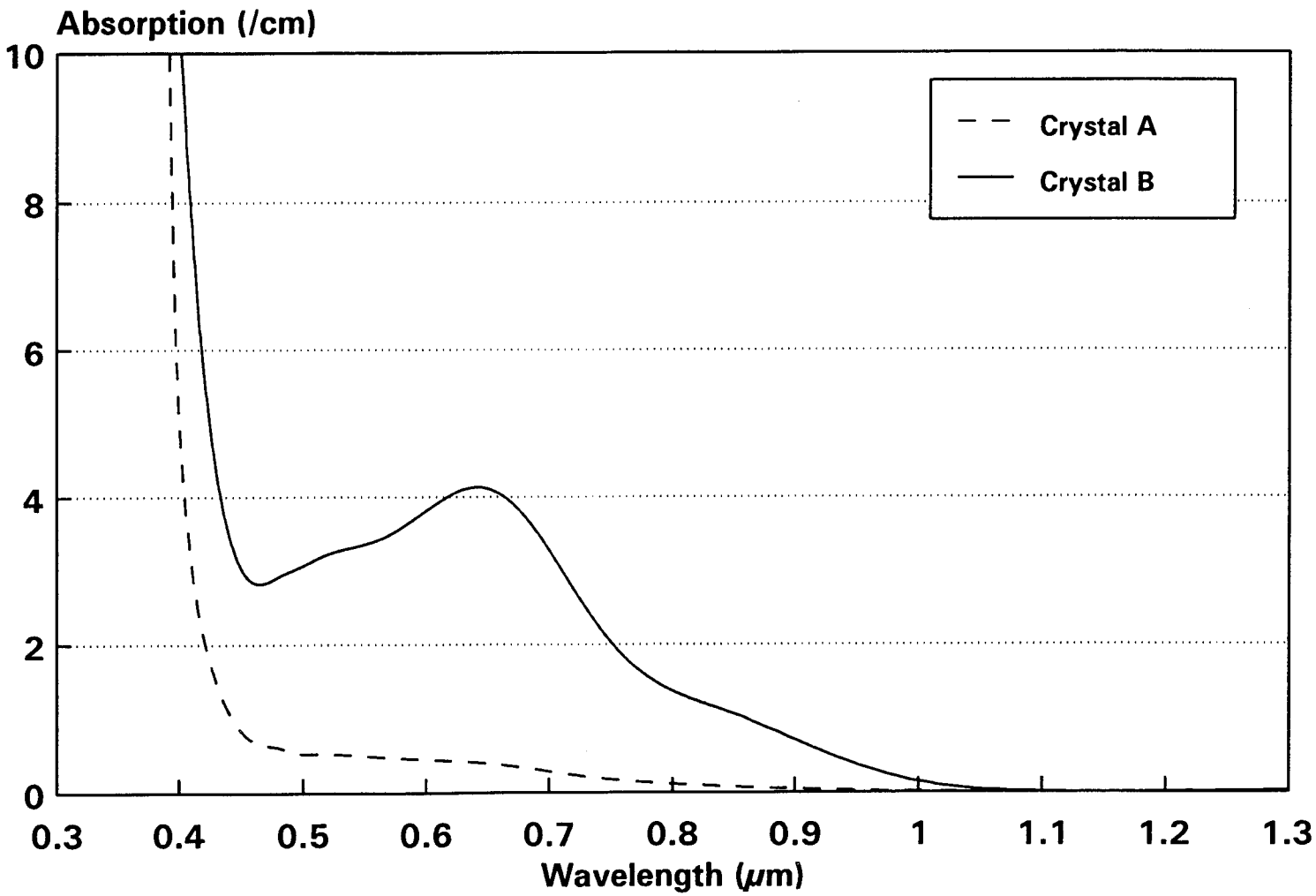
Absorption (/cm)
10
8
6
4
2
0
0.3
0.4
0.5
0.6
0.7
0.8
0.9
1
1.1
1.2
1.3
Wavelength (μm)
Crystal A
Crystal B

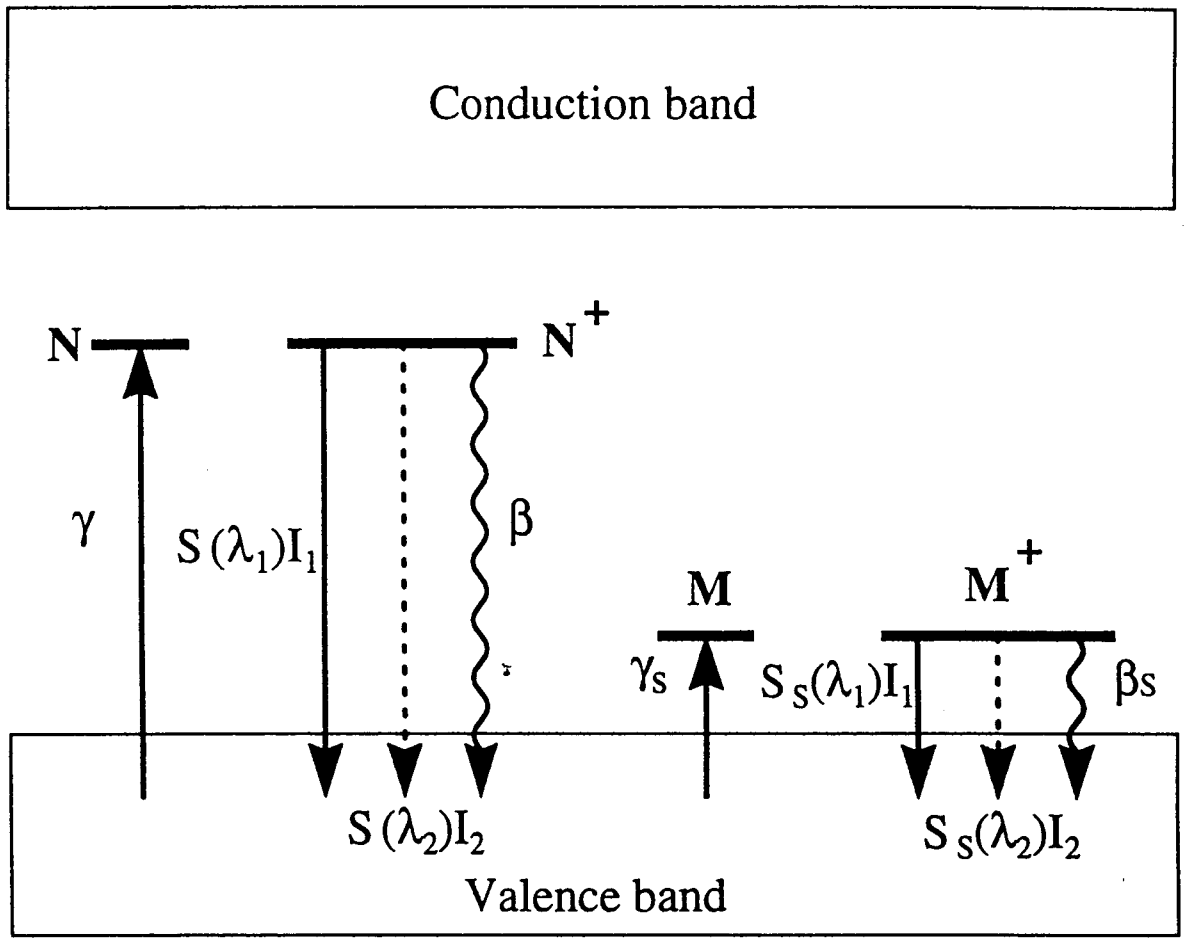
Conduction band
N
N+
γ
S (λ1)I1
β
M
M+
γs
S S(λ1)I1
βs
S (λ2)I2
S S(λ2)I2
Valence band

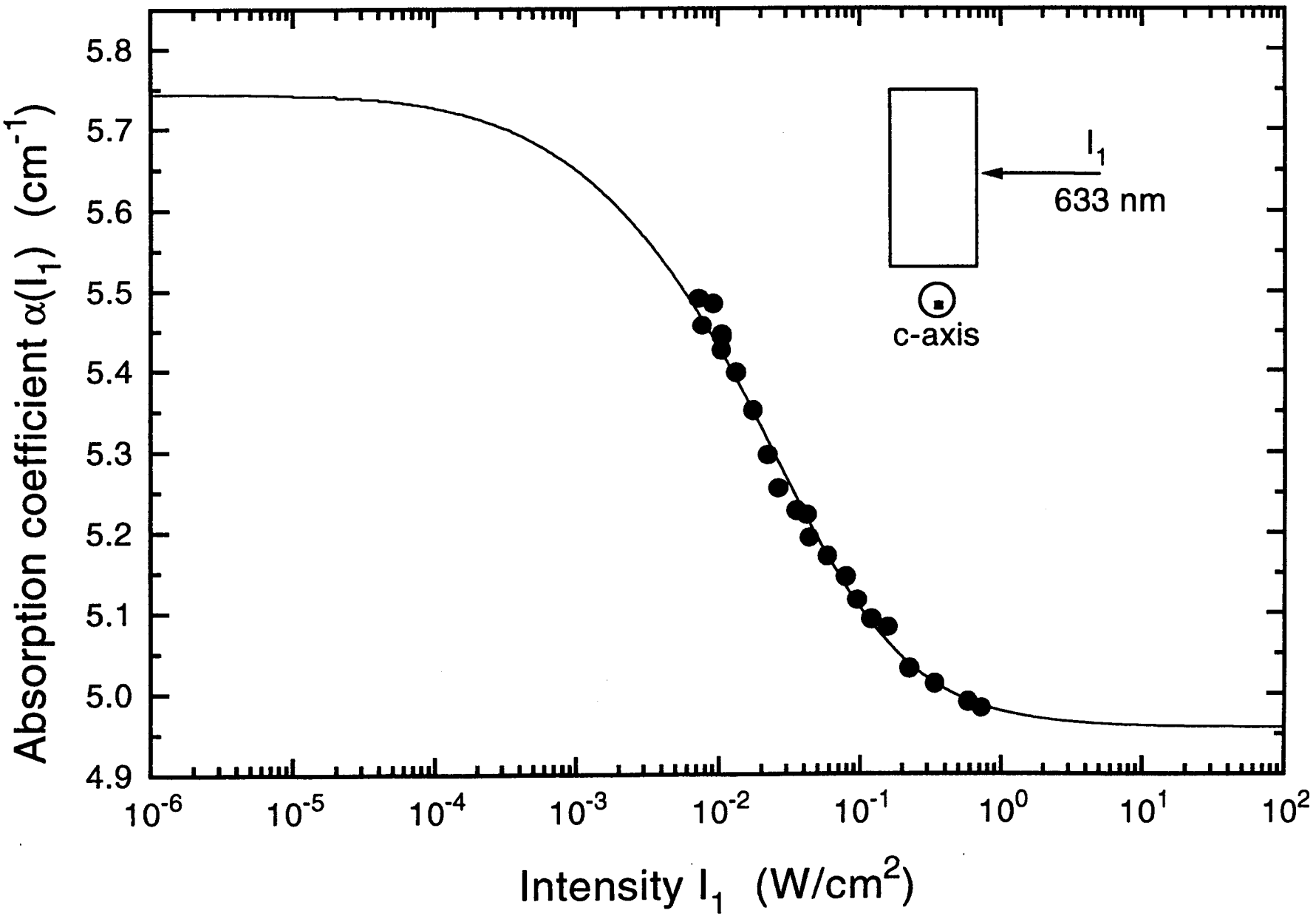
Absorption coefficient $\alpha(I_1)$ (cm^{-1})
5.8
5.7
5.6
5.5
5.4
5.3
5.2
5.1
5.0
4.9
10^{-6}
10^{-5}
10^{-4}
10^{-3}
10^{-2}
10^{-1}
10^{0}
10^{1}
10^{2}
Intensity I_1 (W/cm^2)
I_1
633 nm
c-axis

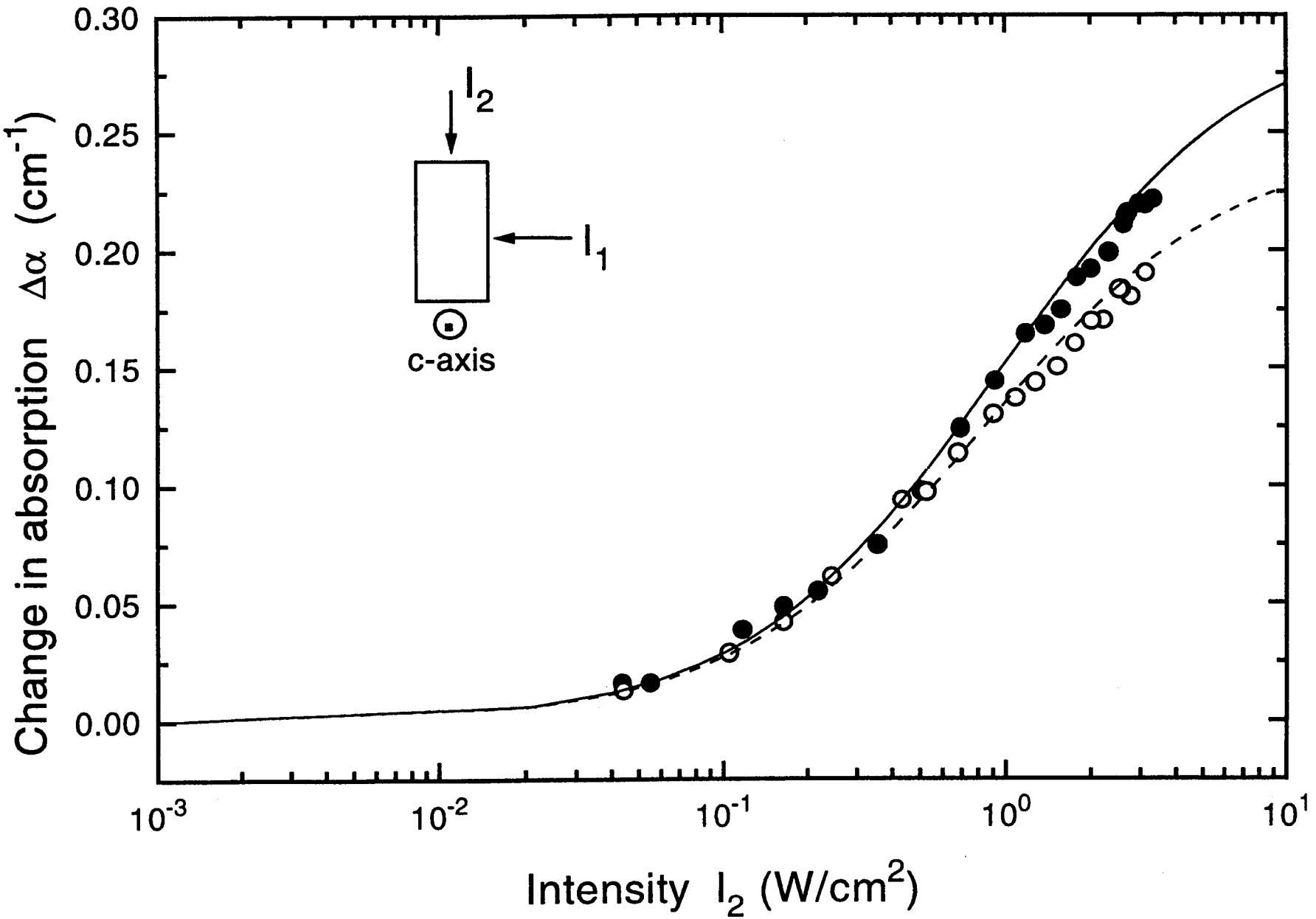
0.30
0.25
0.20
0.15
0.10
0.05
0.00
Change in absorption Δα (cm-1)
I2
I1
c-axis
10-3
10-2
10-1
100
101
Intensity I2 (W/cm2)

TABLE 1. Crystal parameters used in numerical simulations

	Deep centres	Secondary centres
Density of species	$N_D=N+N^+=1.3\times10^{18}\ cm^{-3}$ $N_{dark}=N_D-N_A=2\times10^{16}\ cm^{-3}$	$M_T=M+M^+=1.1\times10^{18} cm^{-3}$ $M^+_{dark}=0$
Photoexcitation cross-section at 633 nm	$S=13.4\ cm^2J^{-1}$	$S_S=2\ cm^2J^{-1}$
Photoexcitation cross-section at 800 nm	$S=5.7\ cm^2J^{-1}$	$S_S=2.2\ cm^2J^{-1}$
Photoexcitation cross-section at 750 nm	$S=7.7\ cm^2J^{-1}$	$S_S=2.4\ cm^2J^{-1}$
Photoexcitation cross-section at 514 nm	$S=8.3\ cm^2J^{-1}$	$S_S=1.8\ cm^2J^{-1}$
Thermal excitation rate	$\beta = 5\times10^{-4}s^{-1}$	$\beta_S = 0.1s^{-1}$
Recombination coefficient ratio γ_S/γ	0.5	